Towards Practical Terahertz Imaging System With Compact Continuous Wave Transceiver

Li Yi ⬤, *Member, IEEE*, Yosuke Nishida, Tomoki Sagisaka,
Ryohei Kaname, *Member, IEEE*, Ryoko Mizuno, Masayuki Fujita ⬤, *Member, IEEE*,
and Tadao Nagatsuma ⬤, *Fellow, IEEE*

Abstract—Terahertz (THz) imaging techniques have attracted significant attention and have developed rapidly in recent years. However, despite several advances, these techniques are still not mature, and their high cost and system complexity continue to limit their applications. In this article, the techniques for achieving a practical imaging system with a compact THz transceiver are addressed, while considering the limitations of the current technique. The aim is to provide a brief review of related topics, while also covering our recent progress, which can provide some general perspectives and contrasting approaches for realizing a practical THz imaging system. The continuous wave devices are mainly focused for their flexibility of balancing the imaging resolution and data acquisition time. The importance of transceiver integration is also discussed and illustrated by introducing a 600-GHz band micro-photonic interface for integrating a THz source and detector, with a single resonant tunneling diode as a transceiver. With regard to system issues, spatial sampling with mechanical beam-scanning is discussed as an intermediate approach for moving stage and array technology. The potential and limitations of this approach are evaluated, along with an elliptical reflector as an alternative to an f-theta lens owing to its low cost and simplicity. The combination of integrated devices, along with the mechanical beam-scanning, is also discussed for demonstrating our current concept of realizing a practical THz imaging system.

Index Terms—Continuous wave imaging, integrated device, mechanical beam-scanning, resonant tunneling diode, THz imaging, THz transceiver.

I. INTRODUCTION

IN RECENT years, a variety of sensing applications in the terahertz (THz) band have attracted significant attention as these frequencies provide sub-millimeter-level resolution and good transparency to electrical insulators such as paper, glass, and polymers. THz imaging techniques can image not only the precise two-dimensional (2D)-distribution of the target of interest but also three-dimensional (3D)-information such as layers, cavities, and adhesive joints. The precise THz image is crucial for a variety of applications ranging from nondestructive testing (NDT) and security to medicine, food inspection and agriculture [1]–[10]. However, the technical difficulties and high costs involved in scaling up these techniques for industrial use have restricted them to laboratory demonstrations [5], [10]. In order to improving the THz imaging technique, many significant works have been proposed for summarizing the related topics from different angles such as imaging speed [7], high-resolution imaging [1], [10], THz array integration [8], [11], [12] and specific techniques [3], [6], [13], while this article mainly focuses on the techniques that will lead to a practical THz imaging system, which includes a compact transceiver and cost-effective spatial sampling method.

For imaging techniques that include the THz band, two different approaches are mainly applied—pulse and continuous wave(CW) imaging. The pulse-based imaging technique, which refers to THz time-domain spectroscopy (TDS), is mainstream for THz sensing/imaging applications [4], [5], [7], [13]. The pulse, with a bandwidth of a few THz, can be used to obtain the pulse duration of picoseconds-order, which further measures the thickness of thin layers to the nearest micrometer, and/or can be used for precise 3D imaging with tomography techniques [14]. While the drawbacks of the pulse system include bulky source device, complicated time-domain data acquisition and its high cost [13].

Compared to pulse, the CW technique usually yields limited bandwidth while it is a more flexible approach for realizing a compact THz imaging system. THz waves can be generated via both photonic and electronic techniques. Moreover, the single-frequency or narrow-band THz imaging systems have been demonstrated in real-time for security and/or inspection applications with a sub-millimeter resolution [1], [3], [6], [10], [15]–[18]. In terms of 3D imaging, modulated CW signals with frequency sweep can be used with a coherent detection scheme to generate synthetic pulses of high power [19]. This technique is known as pulse compression [20] or optical coherence tomography (OCT) in different societies [21]–[23].

For the prospect of flexibility and adaptivity according to the variants of the imaging requirement, we believe that the tunable frequency range of the CW source opens up possibilities in

Li Yi, Tomoki Sagisaka, Ryohei Kaname, Ryoko Mizuno, Masayuki Fujita, and Tadao Nagatsuma are with Osaka University, Osaka 560-8531, Japan (e-mail: yi@ee.es.osaka-u.ac.jp; u395229j@ecs.osaka-u.ac.jp; u068976a@ecs.osaka-u.ac.jp; u955300c@ecs.osaka-u.ac.jp; fujita@ee.es. osaka-u.ac.jp; nagatuma@ee.es.osaka-u.ac.jp).

Yosuke Nishida is with Research and Development Cente, ROHM Company, Ltd., Kyoto 615-8585, Japan (e-mail: yosuke.nishida@dsn.rohm.co.jp).

striking a balance between the imaging resolution, cost, and data acquisition time. For example, a certain frequency bandwidth for 3D imaging can be achieved with a tunable CW technique, and the frequency sweep speed defines the imaging resolution within a required data acquisition time [24]. Furthermore, a compact transceiver can greatly contribute to the practical installation of a THz imaging system [8], [11], [12]. The limited bandwidth makes it possible to guide the THz within the medium, which can lead to a compact device by integrating the THz source and detectors together. Together with the rapid development of THz-band wireless communication techniques, compact THz CW devices at lower THz band are becoming more efficient in terms of performance and price [3], [8]. However, it is still an expensive technology and it is more difficult to implement at or above 300-GHz band with only electronic techniques [25]. Nevertheless, it is expected that the combination of electronic and photonic technique can achieve a compact THz transceiver at different frequency bands for different applications [3], [26].

On the other hand, since a fixed transceiver pair yields only a single pixel, spatial sampling is another key issue for THz imaging systems; the methods used for spatial sampling significantly affect the size, data acquisition time, and cost of the system. In general, both beam-focusing with quasi-optic components and digital focusing techniques such as holography [27], [28] or synthetic aperture radar (SAR) [1], [29]–[31] can be applied to 2D and/or 3D imaging with sufficient spatial sampling. Quasi-optic systems provide high resolution defined by diffraction-limit [32], [33], while the imaging distance is fixed by the focal length of the lens. Hence, they are typically combined with a mechanical beam-scanning system 2D imaging [7], [15], [34], [35]. In contrast, the digital focusing method can be applied to obtain 3D images without a lens [19]. However, this technique is more expensive on account of spatial sampling since a certain frequency bandwidth need to be sampled simultaneously.

THz arrays are expected to offer optimal solutions for simplifying the spatial sampling both imaging approaches introduced above. However, the technical difficulties and costs involved with this technology are prohibitive. Furthermore, most existing THz arrays only include detectors, while an extra source is still required [1], [7], [25], [36]–[39]. In addition to using the array technique, a tunable THz CW transceiver with a scannable quasi-optic system is not without its drawbacks but is a sufficient choice for realizing a practical THz imaging system for 3D imaging [24]. Besides, the efforts on variants of intermediate solutions for achieving a practical THz imaging system should be noted. It is important for users to consider the trade-off between the spatial resolution, which means wider bandwidth, and data acquisition time for the best fits of their requirements.

The recent advances in THz imaging using CW devices at different frequency bands is briefly discussed, in Section II A. Since transceiver integration above the 300-GHz band still involves several problems, such as large losses and limited bandwidth of the waveguide, the concept of integrating the electronic and photonic components is introduced as an effective approach in this frequency band. This is illustrated by the examples of an integrated silicon micro-photonic unit operated at the 600-GHz band [40]. Instead of a conventional integration method, a further

integrated resonant tunneling diode (RTD) transceiver device will also be addressed as an alternative integration technique for reducing the system cost [41]. To arrive at a balance between cost and data acquisition speed, systems that use mechanical beam-scanning are mainly addressed in Section III. A simplified quasi-optic system with only one elliptical reflector is demonstrated together with a single RTD for realizing a cost-effective 2D imaging system [42]. The last section provides a conclusion and prospects for terahertz imaging techniques for related applications.

II. INTEGRATION OF THz TRANSCEIVER FOR IMAGING

A. *THz Sources and Detectors for Imaging System*

The THz transceiver, including the source, detector, and interface components, is a key constituent of the imaging system. As mentioned in the above section, tunable CW devices at different THz bands can contribute to such systems of different requirements. This section focuses on CW sources and their overall integration because they are relatively dominant in the performance of a transceiver, where a general overview of the devices introduced in the following are summarized in Table I.

In general, electronic and photonic devices can be configured to generate CW signals below and above the 300-GHz band, respectively. Multiplication of millimeter waves (MMW) is commonly performed in THz imaging experiments; although the equipment involved is expensive, the refined technique offers better bandwidth and increases power output by the order of a few milliwatts [18], [21], [23], [24], [29], [43]. A well-calibrated system can be directly applied for 3D imaging, as an example, a vector network analyzer operated at the 300-GHz band demonstrated sub-millimeter resolution at a distance of $\sim$2 m by lens-free digital focusing [29].

Electronic devices that can directly generate THz signals with DC bias are cost-efficient for imaging at specific frequency bands, making them a primary contender for large-scale applications and integration. Diodes such as impact-ionization avalanche transit time (IMPATT) diodes [44], Gunn diodes [45], [46], and RTDs [41], [47] have been applied for imaging application. Recently, tunable THz IMPATT sources with power ratings as high as 30 mW and frequency bandwidth of $\sim$30 GHz have been commercialized. It can be expected that similar systems such as the GB-SAR [48] at the MMW band will soon be available in lower THz band; this could provide extraordinary spatial resolution at a stand-off distance. As mentioned in the previous section, significant research into THz imaging arrays with integrated sources and detectors at the 300-GHz band has also been conducted with transistor devices such as heterostructure bipolar transistors (HBTs), high electron mobility transistors (HEMTs), and silicon complementary metal–oxide semiconductor (CMOS) transistors [8], [11], [25], [38], [49]–[53]. We believe that the array technique represents the future trend of THz imaging; however, breakthroughs are required to reduce the cost and develop it beyond the 300-GHz band.

The photonic method plays a major role in obtaining THz signals at higher frequencies. Semiconductor single-oscillator

TABLE I
OVERVIEW OF SOME COMMONLY APPLIED CW THz SOURCES FOR IMAGING PURPOSE

	Operated frequency	Bandwidth	Output power	Transceiver size	Drawbacks
MMW multiplication	< 1 THz	Medium	High	Medium	Not practical for the high cost
THz diodes, transistors	< 1 THz	Narrow	Low/Medium	Compact	Most devices limited below 300-GHz
Photomixing	0.1 – 4 THz	Wide	Low	Medium	Weak power, require extra laser devices
QCL	1 – 5 THz	Narrow	High	Compact	Relatively narrow bandwidth, low temperature required

THz quantum cascade lasers (QCLs) [6], [16], [39], [54]–[56] and photomixing techniques have been investigated for imaging applications. QCLs have the potential for integration [39], [56] and can also provide relatively high power output on the order of milliwatts at frequencies beyond 1 THz; they are hence considered suitable for higher frequency bands. The operational requirement of low temperatures does limit the practical application of QCL; however, recent progress has been made in room-temperature imaging with a QCL device [55].

Photomixing is one of the most promising ways to fill the gap at the 600-GHz band for its wide bandwidth and low phase noise, which is considered to be the next step in high-speed THz wireless communication [3], [26], [57]–[59]. It requires two lasers of different frequencies to be combined into a photomixer, which then yields an output wave signal whose frequency equals the difference between the two input frequencies. The uni-travel carrier diode (UTC-PD) is a promising photomixer for its wide bandwidth and relatively high output power [60]. A huge advantage of CW techniques is that they provide tunable frequencies that range from 0.1 THz to a few THz, which can be used to measure thickness on the order of a few micrometers as THz pulse system [16]. Owing to the high-speed sweep of the laser, the combination of the frequency modulated continuous wave (FMCW) technique with photomixing is a promising method for fast 3D imaging systems in the THz band [59]. Although the bandwidth is limited, device integration with the electronic interface provides possibilities of combining photomixers with electronic devices such as pre-amplifiers [60], [61]. This suggests that photomixing has the potential to be a flexible imaging transceiver and to balance the requirements of imaging resolution and data acquisition time.

There are many kinds of THz detectors available, categorized into photon detectors and thermal detectors [36], [37]. Regarding the data acquisition time, sensitivity, and cost, only a few of them are considered to be mature technologies, i.e., they are developed experimentally and have yet to be commercialized.

For thermal detectors, microbolometers and pyroelectric devices are commonly used in THz imaging experiments and commercial products [36], [38], while for photon detectors, technologies employing silicon CMOS circuits [8], [25], [38], [39], [49], [50], III-V HEMTs [62], [63], Schottky barrier diodes (SBDs) [3], [43], [45], etc., are more mature and used in a variety of integrated devices.

B. Integration of THz Transceiver

1) Integration At 600-GHz Band with Micro-photonic Interface: Imaging cannot be performed with only the transmitter and
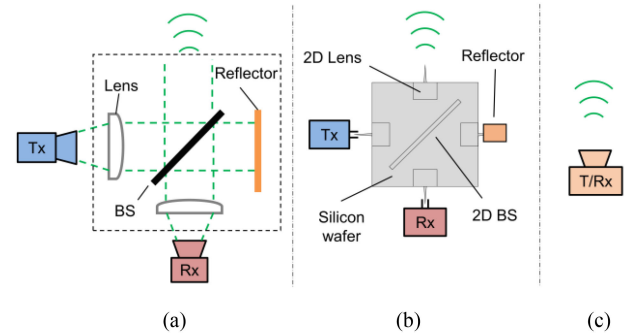

Fig. 1. Concept of simplifying a THz transceiver, Tx indicates a THz source, Rx indicates a detector and BS refers to beam splitter; (a) indicates a quasi-optic configuration for detecting the coherent signal from target and reference mirror; (b) is the integration of quasi-optic within the dashed line of (a) into a 2D silicon wafer; (c) is the idea case of transceiver integration that combines source and detector together with a single device.

receiver—the interface that links the THz wave is also crucial. It helps to detect the transmitted and reflected signals separately, or to detect the coherent signal using a mixer, to obtain range information [19]. The metallic waveguide is a mature technique for the microwave/MMW band; its design is key for the 300-GHz band Si-CMOS integration technique [64]. However, metals exhibit non-negligible ohmic loss in the terahertz range. This is exacerbated by the surface roughness of the internal conductor, as it is challenging to accurately machine a microstrip line of such miniature dimensions [65].

The unlimited frequency bandwidth in free space is the primary reason for the popularity of the quasi-optical configuration in demonstrating THz imaging systems at higher frequency bands, even though they make the systems bulky [1], [3]. A common setup of a quasi-optic system with a THz transceiver and a designed beam splitter is shown in Fig. 1(a). The focus lens operates as waveguides to collimate THz beams on the spatial domain. A reference reflector can reflect the THz beam for coherent detection, while it is also possible to use an absorber here when only the direct detection of signal amplitude is required. Such systems are usually bulky and require precise alignment, which makes them impractical. A simplification of the THz transceiver is, therefore, definitely required. For example, 2D integration as it is shown in Fig. 1(b) is a straightforward way for achieving it with silicon micro-photonic material instead of simple metallic striplines. Fig. 1(c) represents an ideal case of integration, where all the individual components are replaced by a single device.
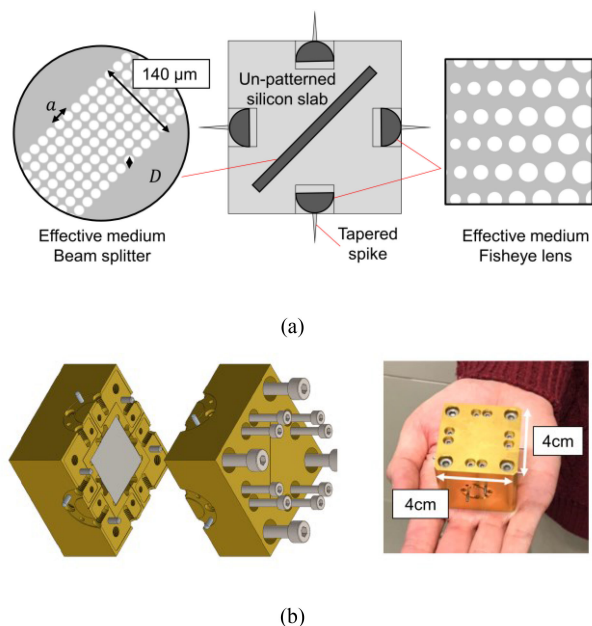
(a)

(b)

Fig. 2. (a) Integrated 2D quasi-optic unit with beamforming functionality of Maxwell fisheye lens and beam-splitter; (b) design of metal package for integrated photonic unit.

Microstructured all-intrinsic-silicon photonic-crystal technology has been developed as an alternative [66]. Devices of this sort achieve field confinement by means of the photonic bandgap in the in-plane direction and the total reflection in the perpendicular direction. This yields highly efficient THz range waveguiding, but this comes at the expense of reduced bandwidth. To address this issue, we employ the same material as that of the aforementioned terahertz photonic crystal devices— high-resistivity silicon—so that it has low losses. However, it is microstructured in a different manner, rather than a photonic crystal, to realize an effective medium. Thus, this material change can accomplish both high efficiency and an ultra-wide frequency bandwidth.

As shown in Fig. 2(a), the integrated unit uses an unpatterned silicon slab and monolithically integrates four half-Maxwell fisheye lenses with a beam splitter. The lenses serve to launch the terahertz wave into the dielectric slab in the form of a confined beam, which is free to propagate within the 2D plane of the slab. The wave propagation is identical to the conventional quasi-optic configuration introduced previously, while a terminator or an isolator can be applied instead of reference reflector or absorber to 3D and 2D imaging, respectively.

The core idea for designing the lenses and beam splitter is the implementation of an effective medium. This is composed of a subwavelength through-hole array that mixes air into a silicon slab. A terahertz wave experiences this structure as a homogeneous medium of effective index that is mediated by the filling factor of air in silicon; larger through-holes produce a lower index. A Maxwell fisheye lens is a radially symmetrical optic that maps a point source to a diametrically opposed focus, as indicated in Fig. 2(a). This lens converts a point source at its focus to a plane wave that is projected normally from its bisecting

line segment. As the structure is entirely passive, this operation is bidirectional. The lens is fed by an all-dielectric waveguide coupled directly to its focus. The concept of lens design was previously established in [67].

The beam splitter which is also shown in Fig. 1(a) is another important integrated 2D components. Subwavelength through-holes are arrayed in a diagonally oriented square lattice, thereby forming an effective medium. This produces a local discontinuity in the effective index, which causes reflection within the slab. The intended functionality of the beam splitter is to evenly divide the incident radiation between the transmitted and reflected waves, as this yields the highest possible signal-to-noise ratio when used in an imaging system. The ratio between transmitted and reflected powers can be designed by adjusting the width of the beam splitter, period of the holes a, and diameter of holes D. Considering Fabry–Perot interference, the width of the beam splitter is set to 140 µm because its bandwidth is approximately 500–700 GHz, which is suitable for application to 600-GHz band imaging systems. While a and D were optimized via simulation for 23 and 15.6 micrometer, respectively. The details evaluation can be found in [40], while some imaging results and the imaging system are introduced in Section III-A.

For practical use, packaging structures are necessary to house fragile microstructured silicon units. To this end, a metal case was designed and fabricated. Fig. 2(b) shows the cross section of the metal case, in which four waveguide parts are designed to connect with the coupling spikes of the integrated unit. A cross-shaped trench was cut into the bottom of the trench under the portions of the silicon unit that carries terahertz waves. Thus, the metal components are separated from the wave propagation part by more than 2 mm; hence, these metal components have no influence on wave propagation [68]. Metal pins and threaded holes are incorporated onto the sides of the case to facilitate physical coupling with hollow metallic waveguides that are terminated with a standard UG-387/UM flange to facilitate connection with external equipment.

2) Integration to a Single Device: As shown in Fig. 1(c), the ultimate form of a THz transceiver comprises an integration of the source, detector, and interface components. The integration of devices for performing THz imaging is therefore highly desirable as it can ultimately allow the production of convenient, compact, and potentially mass-producible low-cost equipment for practical applications. In addition to using the 300-GHz-band CMOS integrated techniques that actually link the transmitter and receiver on chip [8], [52], [64], the QCL source has been successfully integrated with the SBD receiver monolithically for imaging purposes [56].

As another approach, some special devices can realize transceiver integration directly with their inherent features. It is demonstrated that the QCL itself can be used directly as a transceiver with its self-mixing property [6], [69]. For electronic devices, a security application is demonstrated with commercialized sub-harmonics mixer at the 300-GHz band as a transceiver that uses a leaked LO signal as the THz source. Although the output power was only a few microwatts, a hidden weapon model could be detected at a distance of ∼8 m distance [70].

As introduced in Section II A, RTD is an electronic device that can operate as both a THz source and detector at room temperature [71]. Its oscillation at ∼2 THz has been reported in [72], while a detailed study on RTD receivers was reported for the 600-GHz band [73]. The RTD operation is determined by its current–voltage (I–V) characteristics. In the negative differential conductance (NDC) region, due to the quantum tunneling effect, oscillation occurs if the magnitude of the NDC exceeds the positive conductance of the resonator circuit. Recently, an RTD oscillator exhibits extraordinary sensitivity as a coherent detector when it operates as a self-oscillating mixer. Hence, the RTD device is applied for homodyne wireless communication in the 300-GHz band without using an extra LO source [74]. When the RTD is biased in the NDC region, the RTD can simultaneously provide LO signal while operating as a mixer. Moreover, a single RTD can be employed as both transmitter and receiver simultaneously for imaging applications. When the RTD operates in the NDR region, a small portion of the self-oscillating signal remains within the RTD device as the LO signal, while most of the self-oscillating signal is transmitted and reflected at the target, denoted as the reflected signal. Because the transmitted and received signals are at the same frequency, injection locking can occur, resulting in signal detection with low phase noise [73], [75], [76].

The reflected signal acquires a constant phase shift of $2\pi f \frac{2d}{c}$ during propagation, where d is the distance to the target, f is the oscillating frequency of the RTD, and c is the speed of light. If the high-frequency components of the detected signal are removed, the remaining detected voltage V_{LPF} can be expressed as (1), and a similar result can also be obtained by considering the mechanism of the external feedback property of the RTD [77].

$$V_{LPF}(t) \propto A cos\left(\frac{4\pi f d}{c}\right) \qquad (1)$$

Equation (1) indicates that when the oscillation frequency is swept or the distance to the target is linearly varied, the detected signal becomes a cosine function that can provide accurate range information.

For confirmation, we performed ranging measurements to demonstrate the capability of the RTD transceiver sensor. The experimental setup of the imaging experiment employing the RTD transceiver module is shown in Fig. 3(a). The applied RTD is integrated within a hollow waveguide with a standard UG-387/UM flange and its concept is shown in Fig. 3(b). The output power was ∼50 μW, and the oscillating frequency was ∼278 GHz with a bias voltage of 0.71 V. The schematic diagram of the system is shown in Fig. 3(c). The transmitted signal was spatially modulated by an optical chopper with a frequency of 1 kHz and then transmitted to a mirror at a distance of 32.5 cm. The reflected signal was output via the bias tee and a lock-in amplifier, and an analog/digital (A/D) converter was used to digitalize the signals. A mirror reflector mounted on the moving stage was moved toward the RTD module, and the detected phase differences were evaluated. When the mirror reflector shifted 3.5 mm, and a clear periodical signal can be obtained, as shown in Fig. 3(d). The wavelength was 0.54 mm, which corresponds to the oscillation frequency of the RTD. Owing to
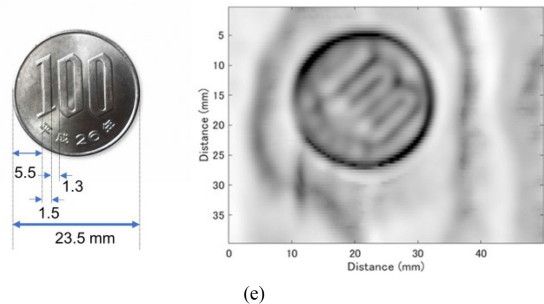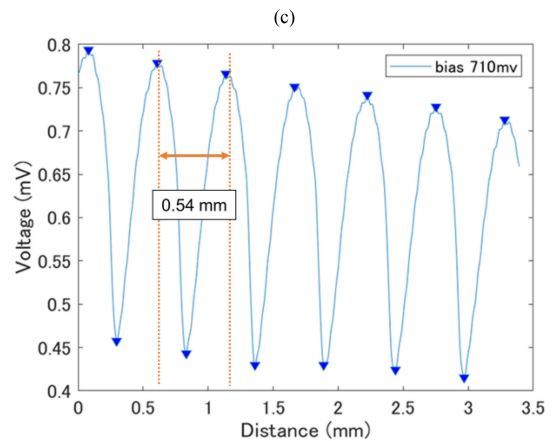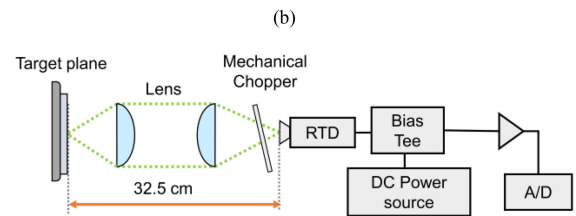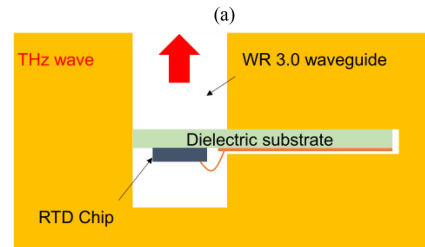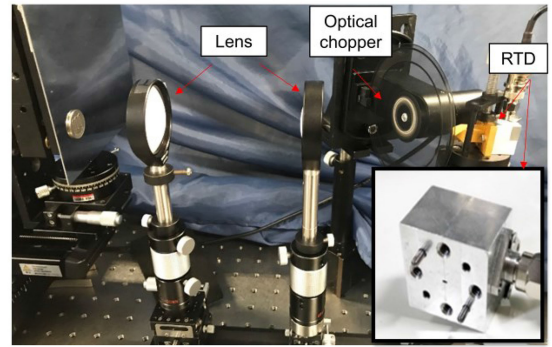

Fig. 3. Demonstration of a single RTD transceiver for imaging application; (a) Experiment setup; (b) concept of the waveguide integrated RTD (b) block diagram of experiment setup; (c) coherence signal obtained by moving the reflector; (d) imaging result of a 100-yen coin, ∼ 1 mm spatial resolution can be obtained.
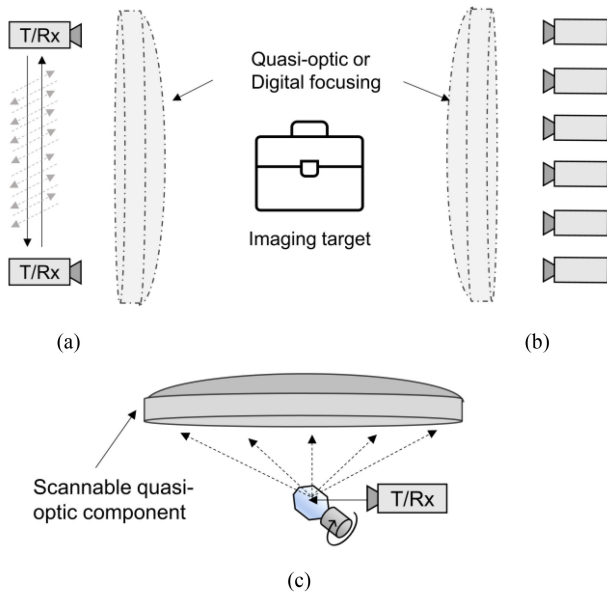
Fig. 4. Methods of spatial sampling for THz imaging, T/Rx indicates a transceiver; (a) indicates spatial sampling by moving a transceiver; (b) represents array concept which requires multiple transceivers; (c) indicates the mechanical beam-scanning approach by changing the beam direction.

the low phase noise of such a configuration, a resolution of less than 4 µm can be realized by detecting the voltage variation of the detected signal without using an extra amplifier. Furthermore, a 100-yen coin inside the envelope (the envelope was not included in Fig. 3(a) for recognizing the position target) was imaged at a distance of ∼20 cm with the conventional quasi-optic setup shown in Fig. 3(a) and a 2D moving stage. The spatial resolution of ∼1 mm was measured experimentally by using knife edge method [42]. The text on the surface of the coin could be imaged clearly as it is shown in Fig. 3(e).

Such simplified integration devices can greatly reduce the system cost and have the potential for specific applications. As reported in [41], similar experiments have also demonstrated with a RTD integrated with micro-photonic interface. On the other hand, narrow bandwidth of ∼ 20 GHz can also be obtained by changing the bias voltage of RTD oscillating at 300-GHz band, although such operation is still not stable, it opens the possibility for 3D imaging. Besides, the RTD transceiver can further be applied for holographic imaging [27] or Doppler detection [78], which do not require large bandwidth.

III. SPATIAL SAMPLING FOR A PRACTICAL IMAGING SYSTEM

A. Approaches for Achieving Efficient Spatial Sampling

As described in Section I, spatial sampling is a key aspect in THz imaging systems. The spatial sampling by using moving stage which is shown in Fig. 4(a) is a straightforward and convenient way for experimental studies which requires only one transceiver device. However, a spatial sampling interval of at least half a wavelength is required according to the Nyquist sampling criterion, which means a 0.5-mm sampling interval is required for the 300-GHz case. Under such conditions, the RTD

imaging of the 40 × 40 mm area shown in Fig. 3(d) required a few minutes for data acquisition. Extra efforts are necessary to handle such dense data sampling in a short time to realize real-time THz imaging.

For consideration of research and future trends, it is evident that the array system together with beam-forming technique which is shown in Fig. 4(b) can finally lead to a real-time imaging system [7]. Since there are always limitations for mechanical operation, performing digital processing with multiple sensors is still the final objective for solving the problem of spatial data sampling. As it is discussed in Section II-A, although integrated transceiver array systems are limited at the 300-GHz band, THz detector arrays, which are also defined as THz cameras, are based on relatively mature techniques [7], [45], [62], [79]. Owing to the high cost and limitation of the directional THz beam, the current devices can only image a small area, hence the combination of a linear array with a quasi-optic system is also an effective way to further enhance the imaging speed while achieving a larger survey area [37], [45], [79].

In addition, some other novel techniques from the MMW society and the optic society have also been applied for fast THz imaging. A leaky wave antenna was recently introduced to the THz band, which uses an antenna device for steering THz beams at different frequencies. It also demonstrated that the SAR technique can be applied for vital signal detection in a specific direction [18]. Similarly, the metasurface technique has been introduced for the THz band for beam steering with a single THz transceiver [80], [81]. The single-pixel imaging based on compressed sensing has also been demonstrated for realizing the real-time THz imaging [7], [82], [83]. The 2D image can be directly obtained with a single THz transceiver without spatial sampling, while additional masks are necessary to obtain the spatial information of the target. Similar to the device integration techniques introduced in Section II-B.2, these novel techniques provide insights for achieving faster imaging or reducing the cost of the system.

It is also worth noting that the conventional moving stages are slow for acquiring THz images, while combining them with the SAR technique allows for a relatively large survey area to be covered in a short time. An impressive 300-GHz SAR system was presented in [19] by moving a transceiver mounted on a vehicle. Such digital imaging techniques without quasi-optic systems require a considerable amount of output power or pre-amplifiers, which currently limits their applicability; however, these techniques can perform 3D imaging without the limitation caused by the focal length of the optical lens. Owing to the small size of THz devices and simple integration techniques, it is possible to use micro-drones to obtain spatial sampling at the required distance and imaging region. Although these techniques are not mature for practical applications, they provide more possibilities for widening the application of THz imaging techniques.

In order to keep the low cost of using single transceiver while enhancing the imaging speed, an alternative way is to reduce the spatial movement of a transceiver by introducing rotating a reflector, then using a scannable quasi-optic component to guide the THz beam for fast spatial sampling, as it is shown in Fig.

4(c). At current stage, it is not without its drawbacks but is a sufficient choice for achieving a practical THz imaging system with a single transceiver.

B. Methods for Mechanical Beam-Scanning

1) Combination of F-Θlens with Integrated Optical Unit: As it is discussed in previous section, mechanical beam-scanning is still a cost-efficient method at the current stage. The use of focusing elements such as an f-theta lens and/or a concave mirror, along with a galvano mirror, has been introduced in many THz imaging systems [46], [54], [84]. This method is suitable for inspection applications when the targets are moving on a conveyor belt, while the imaging speed along the moving direction of the conveyor belt is usually limited to less than 1 m/s owing to the limitation of the rotating speed of the galvano mirror. By introducing a polygon mirror, the scanning speed can be further enhanced [15], [35]. Moreover, 2D imaging of a small region can be obtained with a 2D galvano mirror system and it has been demonstrated with a THz reader [85]. Additionally, a compact imaging system for imaging a small region of ∼8 cm has been reported with using a photomixing source [86]. Besides, the integrated optical unit introduced in Section II-B.1 was constructed by combining the f-theta lens and the galvano mirror for achieving wideband low-coherence imaging at the 600-GHz band.

Fig. 5(a) shows the block diagram of the imaging system that uses an integrated unit. At the transmitter side, a low-coherence signal source is generated by photomixing of 600-GHz carrier signal and amplified spontaneous emission noise of ∼70 GHz bandwidth with an UTC-PD [21]. The use of low-coherence signals can reduce imaging artifacts that arise due to interference effects and improve the quality of the imaging results. On the receiver side, the terahertz signal is detected by an SBD and measured using lock-in detection. The signal in the waste port is radiated to free space by a horn antenna and absorbed by an absorber. The signal that is interfaced with the sample under test is radiated from a horn antenna, collimated by a parabolic mirror, scanned by a galvano mirror, and concentrated by an f-theta lens. Here, the sample under test is moving in a direction perpendicular to the scanning direction. Fig. 5(b) shows a photograph of the imaging system using the integrated unit. It can be observed that the system is much more compact than the conventional quasi-optic lens and beam splitter. Fig. 5(c) shows the imaging result. An envelope made of paper was used as the sample, and a wrench and clip were placed inside the envelope. The choice of sample employed in the imaging experiment is intended to represent a prospective application and the detection of foreign materials. The imaging system employs terahertz waves in the 600-GHz band, exhibiting sub-millimeter resolution and transparency to paper. The wrench and clip, whose widths are approximately 1 mm, can be detected through the paper envelope. It should be noted that the low-coherence imaging technique effectively suppresses artifacts caused by the interference. The broad bandwidth of the integrated unit is beneficial in this regard, thus allowing us to clearly distinguish the wrench and clip in the envelope.
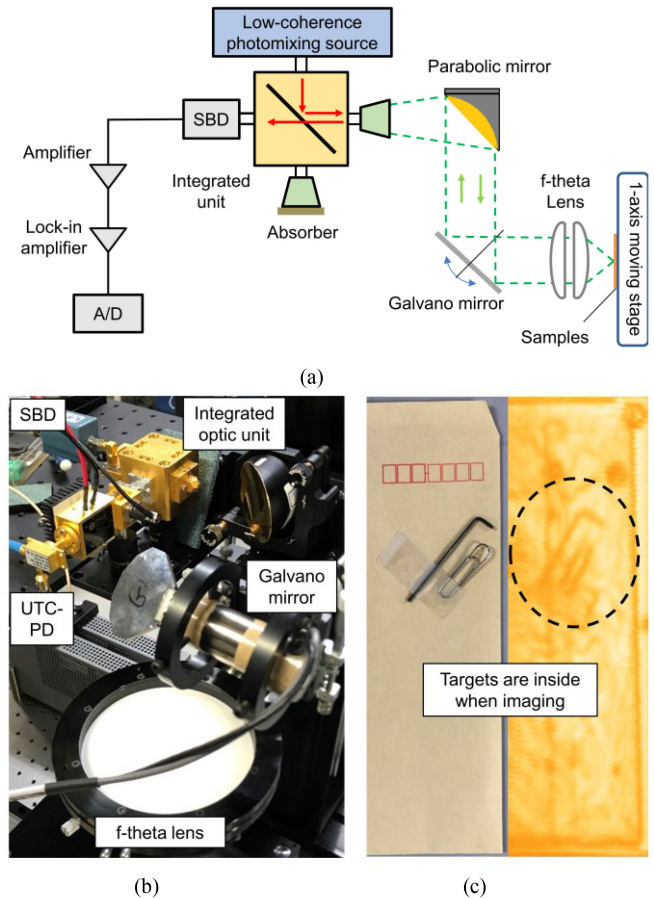

Fig. 5. (a) Block diagram of imaging system using integrated optic unit; (b) experimental setup by introducing integrated unit; (c) imaging result of an envelope with a wrench and clip inside.

2) Simplified Elliptical Reflector for Mechanical Beam-Scanning: For practical applications, the dielectric lens for the THz band is still expensive, especially for larger imaging areas, while the metal reflector can be a better choice for reducing the cost and reflection loss. An elliptical reflector was introduced for the 600-GHz band imaging for security applications, and a 25-m imaging distance was achieved by using a well-calibrated beam-scanning system, while the spatial resolution was ∼10 mm due to the long-distance and limited bandwidth [87]. Similar systems at 300-GHz band were reported and summarized in [88], for a achieving faster data acquisition speed. Although multiple reflectors are applied for covering the reduced spatial resolution caused by the beam-scanning, most of the results obtained the spatial resolution as much as 5-10 times the operating wavelength. Another method of using an elliptical reflector is to combine with digital focusing, which is proposed in [89], [90] for security applications. This reflector focuses the beam in only one direction while signal processing is used for focusing the beam in the perpendicular direction. It shows a better spatial resolution of ∼4 mm at the 200-GHz band, which is about 2 times its wavelength. Recently, another strategy is proposed for designing an alternated elliptical reflector that can focus the beam in both directions without extra signal processing. It is
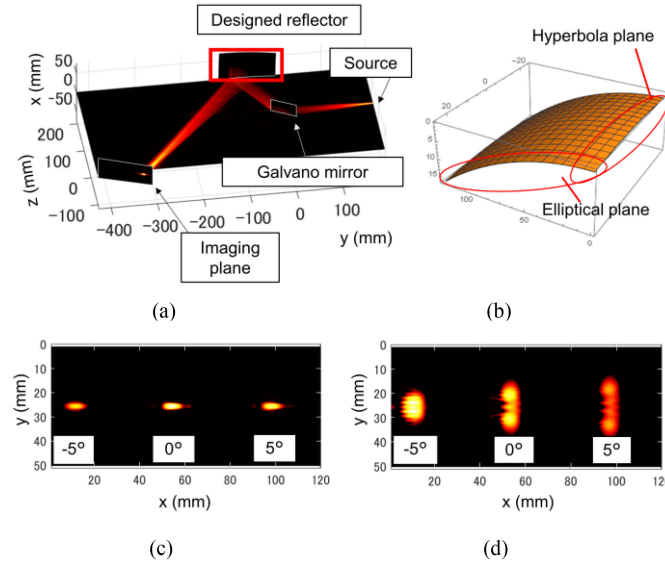
(a)

(b)

(c)

(d)

Fig. 6. (a) Propagation path simulation of designed system; (b) surface of the designed elliptical reflector; (c) simulation results of focused beam at different rotation angle with proposed elliptical reflector; (d) simulation results of focused beam at different rotation angle with conventional elliptical reflector.

(a)

(b)

(c)

(d)

Fig. 7. Combination of designed elliptical reflector and RTD transceiver for 2D imaging; (a) block diagram of the imaging system (b) experiment setup of the system;(c) imaging target of a T shape absorber attached on a mirror reflector; (d) imaging result.

featured for its simplicity as only one reflector is required for achieving a spatial resolution of ∼0.7 mm at the 600-GHz band.

Fig. 6(a) shows the beam propagation configuration with designed reflector. The source is placed at a specific location away from the focal point of elliptical plane for achieving a balance between spatial resolution and linearity of beam-scanning. The concept of the proposed reflector is illustrated in Fig. 6(b) indicates that the designed concave mirror is shaped as an anamorphic surface, wherein the elliptical plane and hyperbolic plane are designed and merged at perpendicular directions. Such surfaces can be mathematically defined as

$$z = \frac{x^2/R_x+y^2/R_y}{1+\sqrt{1-(K_x+1)x^2/R_x^2-(K_y+1)y^2/R_y^2}}, \quad (2)$$

where x, y, and z are the surface coordinates; K_x and K_y are the conic constants in the x and y directions, and R_x and R_y are the curvature radii in the x and y directions, respectively. The conic constant defines the shape of the surface; for example, when $0 < K < 1$, the surface shape becomes an elliptical plane, and when $K < -1$, the surface shape becomes a hyperbolic plane. When the source is away from the focal point, beam steering can be achieved by changing the beam direction with a galvano mirror [91]. However, a trade-off exists between spatial resolution and scanning region [87]. Then, the elliptical plane was first adopted for the horizontal axis, and the shape of the vertical axis was adjusted to a hyperbola. The designed surface was optimized using numerical simulation, and the parameters were selected as $K_x = -3.6$, $K_y = 0.55$, $R_x = 328$ mm, and $R_y = 472$ mm. Fig. 6(c) and (d) compare the simulation results of the focused beam at different reflection angles with the designed elliptical reflector and a conventional elliptical reflector. The source points for both mirrors were placed away from the focal point for scanning. It is seen that the focused
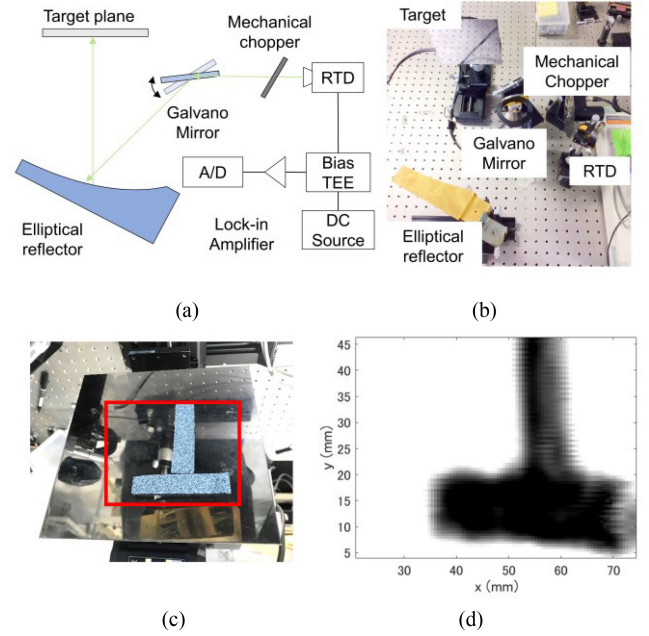
beam size of the designed concave mirror is much smaller than that of the conventional ellipsoid mirror, which corresponds to the experimental results of horizontal and vertical resolutions of ∼2 and ∼0.7 mm, respectively [42]. The designed elliptical reflector supports an imaging speed of 0.1 m/s with an imaging width of ∼12 cm.

By combining the designed reflector with the RTD transceiver introduced in the previous section, a simplified imaging system is presented in Fig. 7. The system configuration is shown in Fig. 7(a), the setup of the transceiver side is similar to that shown in Fig. 3(b). An extra galvano mirror is applied for the mechanical beam-scanning together with the proposed elliptical reflector. The system is experimentally installed, as shown in Fig. 7(b); its components are very simple, and it can be redesigned to be a compact imaging system by reducing the imaging range. As shown in Fig. 7(c) and (d), a simple T-shaped absorber can be imaged clearly by moving the target perpendicular to the beam-scanning direction.

As mentioned in the Introduction section, 3D imaging is always required for THz imaging. However, there is currently a gap between time-consuming 3D data acquisition with the TDS technique and real-time 2D CW imaging techniques. For some specific cases, only millimeter-thick-layer targets need to be imaged separately, such as for the inspection of packaged electronic devices. The combination of CW frequency sweeps with a scannable reflector can be a cost-efficient approach. Previously, such systems were realized with electronic radar techniques, where only the centimeter order range resolution were achieved due to the limited bandwidth [24], [87], [89].

With the advances of accessing wider bandwidth for 3D imaging, some applications was demonstrated with the designed elliptical reflector [42]. A THz tag consists of two-dimensional photonic crystal slabs placed in a matrix, where each slab has its own absorption frequency [85]. By applying the frequency sweep from 450 to 750 GHz along each pixel on the THz tag, the 2D tag information can be obtained corresponding to both spatial distribution and frequency absorption distribution of a specific tag. With the same configuration, thickness measurement of a 1 mm-thick acrylic plate is demonstrated with a range resolution of ∼1.4 mm. Currently, MMW multiplier is applied as THz source, hence the acquisition time is slow owing to the limitation of the sweep time when using the synthesizer. The combination of a beam-scanning system with a photonic-based CW sweep is our next objective for advancement in fast 3D imaging with sub-millimeter resolution.

IV. CONCLUSION AND OUTLOOK

THz imaging technology is developing rapidly, but it is still not a mature technology and difficult for large-scale production. Although many applications have been successfully demonstrated with various THz devices and techniques, the high cost and system complexity continue to limit the popularization of THz applications. Among all features of THz imaging techniques, the fast 3D imaging with sub-millimeter resolution is the most significant. However, the trade-offs between the imaging resolution and data acquisition time are the main concerns in designing a practical imaging system. A tunable CW source approach is more flexible and can handle different applications than obtaining micrometer-order resolution with THz pulse. Based on current techniques for real-time 2D imaging with a single frequency, the enhancement of frequency sweep speed within a certain data acquisition time is a steady approach for realizing a real-time 3D imaging system. Photomixing with the CW technique can potentially balance the imaging quality with cost in various manners, such as that observed in low-coherence imaging [21] or by obtaining pulse signals with FMCW for fast 3D imaging [3].

From the perspective of a compact device requirement, the integration of the THz transceiver is a key aspect in realizing a practical imaging system. This is also the first step for implementation of on-chip integrated THz arrays. The THz transceiver array in the band below 300 GHz is being developed rapidly using the CMOS-LSI technique. However, at frequency bands above 600-GHz band, pure electronic techniques face many problems, such as difficulty in signal generation, significant loss in waveguides, and a lack of interface components, such as couplers/dividers. For this purpose, we present a compact photonic unit that aims to integrate electronic components with the photonic interface. As stated in [3], [26], [56], the combination of the photonic and electronic techniques is crucial for further development of THz techniques. Although many issues of electronic devices remained to be solved such as limited oscillating frequency and bandwidth, they are potential for realizing the large-scale production of 3D imaging system with low-cost.

In contrast, although photomixing devices have been integrated with waveguide [60], additional fiber links to the laser device are still required. The further integrated device that includes a semiconductor laser is essential.

To further reduce the cost, some special devices exhibit the potential for integration without the need for separate sources and detectors, and the coherent signal can be obtained directly. Both the QCL and RTD exhibit such properties, and easily facilitate further simplification of the THz imaging system. Despite the bandwidth issue mentioned above, the mechanism of such properties has not yet been clearly explained. The physical exploration of such devices is still underway [73], [92], [93] for generalizing their applications. We believe that a compact transceiver is the key feature of THz device, which make it possible for mounting in different devices such as phones and micro-drone for widening the application of THz imaging techniques.

Because THz arrays are currently difficult to obtain and are expensive, the mechanical beam-scanning is an intermediate method for obtaining THz images in real-time. As mentioned at the end of Section III-A, 3D imaging can be achieved through combination with a fast frequency sweep THz source, and we believe it can be a practical solution for frequency bands beyond 600-GHz by combining with photomixing techniques, which is still difficult for array techniques. Although scannable quasi-optic components, such as f-theta lenses and elliptical reflectors, have been applied and discussed in many studies, problems, such as insufficient spatial resolution, still remain [35], [87]. A major reason for such unresolved problems may be the fact that THz beam can neither be easily collimated nor radiated widely as microwave radiation. Combined with the improvements of the theoretical analyzation of THz propagation and optical component design, the combination of signal analysis and processing techniques can be another solution [94] to such problems. Furthermore, as stated in the previous section, the use of a THz array, in combination with other novel techniques, such as the sparse array concept [95], or combining arrays with a mechanical beam-scanning system for higher data acquisition speed with lower cost, can also be a future trend for solving spatial sampling issues.

REFERENCES

[1] D. M. Mittleman, "Twenty years of terahertz imaging [Invited]," *Opt. Exp.*, vol. 26, no. 8, pp. 9417, 2018, doi: 10.1364/oe.26.009417.

[2] J. F. Federici *et al.*, "THz imaging and sensing for security applications - Explosives, weapons and drugs," *Semicond. Sci. Technol.*, vol. 20, no. 7. 2005, doi: 10.1088/0268-1242/20/7/018.

[3] R. Safian, G. Ghazi, and N. Mohammadian, "Review of photomixing continuous-wave terahertz systems and current application trends in terahertz domain," *Opt. Eng.*, vol. 58, no. 11, pp. 1, 2019, doi: 10.1117/1.oe.58.11.110901.

[4] C. Wang, J. Y. Qin, W. D. Xu, M. Chen, L. J. Xie, and Y. B. Ying, "Terahertz imaging applications in agriculture and food engineering: A review," *Trans. ASABE*, vol. 61, no. 2, pp. 411–424, 2018, doi: 10.13031/trans.12201.

[5] Y. H. Tao, A. J. Fitzgerald, and V. P. Wallace, "Industrial sectors with terahertz technology," *Sensors*, vol. 20, no. 3, p. 712, 2020.

[6] P. Dean *et al.*, "Terahertz imaging using quantum cascade lasers - A review of systems and applications," *J. Phys. D. Appl. Phys.*, vol. 47, no. 37, 2014, doi: 10.1088/0022-3727/47/37/374008.

[7] H. I. G. Uerboukha and K. A. N. Allappan, "Toward real-time terahertz imaging," *Adv. Opt. Photon.*, vol. 10, no. 4, pp. 843–938, 2018.

[8] P. Hillger, J. Grzyb, R. Jain, and U. R. Pfeiffer, "Terahertz imaging and sensing applications with silicon-based technologies," *IEEE Trans. Terahertz Sci. Technol.*, vol. 9, no. 1, pp. 1–19, 2019, doi: 10.1109/TTHZ.2018.2884852.

[9] C. Jansen *et al.*, "Terahertz imaging: Applications and perspectives," *Appl. Opt.*, vol. 49, no. 19, 2010, doi: 10.1364/AO.49.000E48.

[10] D. Nüßler and J. Jonuscheit, "Terahertz based non-destructive testing (NDT)," *tm - Tech. Mess.*, vol. 88, no. 4, 2020, doi: 10.1515/teme-2019-0100.

[11] K. Sengupta, T. Nagatsuma, and D. M. Mittleman, "Terahertz integrated electronic and hybrid electronic–photonic systems," *Nat. Electron.*, vol. 1, no. 12, pp. 622–635, 2018, doi: 10.1038/s41928-018-0173-2.

[12] X. Gao, X. Liu, Z. Dai, S. Li, and W. Liu, "Integrated terahertz confocal imaging system based on THz waveguides," *Hongwai yu Jiguang Gongcheng/Infrared Laser Eng,* vol. 48, pp. 1–5, 2019, doi: 10.3788/IRLA201948.S219001.

[13] J. Neu and C. A. Schmuttenmaer, "Tutorial: An introduction to terahertz time domain spectroscopy (THz-TDS)," *J. Appl. Phys.*, vol. 124, no. 23, 2018, doi: 10.1063/1.5047659.

[14] S. Wang and X. C. Zhang, "Pulsed terahertz tomography," *J. Phys. D. Appl. Phys.*, vol. 37, no. 4, 2004, doi: 10.1088/0022-3727/37/4/R01.

[15] E. S. Lee *et al.*, "High-Speed and cost-effective reflective terahertz imaging system using a novel 2D beam scanner," *J. Light. Technol.*, vol. 38, no. 16, pp. 4237–4243, 2020, doi: 10.1109/JLT.2020.2988890.

[16] L. Liebermeister, S. Nellen, R. Kohlhaas, S. Breuer, M. Schell, and B. Globisch, "Ultra-fast, high-bandwidth coherent CW THz spectrometer for Non-destructive testing," *J. Infrared, Millimeter, Terahertz Waves*, vol. 40, no. 3, pp. 288–296, 2019, doi: 10.1007/s10762-018-0563-6.

[17] P. Zolliker and E. Hack, "THz holography in reflection using a high resolution microbolometer array," *Opt. Exp.*, vol. 23, no. 9, pp. 10957, 2015, doi: 10.1364/oe.23.010957.

[18] H. Matsumoto, I. Watanabe, A. Kasamatsu, and Y. Monnai, "Integrated terahertz radar based on leaky-wave coherence tomography," *Nat. Electron.*, vol. 3, no. 2, pp. 122–129, 2020, doi: 10.1038/s41928-019-0357-4.

[19] M. Caris, S. Stanko, S. Palm, R. Sommer, A. Wahlen, and N. Pohl, "300 GHz radar for high resolution SAR and ISAR applications," in *Proc. Int. Radar Symp.*, 2015, pp. 577–580, doi: 10.1109/IRS.2015.7226313.

[20] L. Battaglini, S. Laureti, M. Ricci, P. Burrascano, L. A. J. Davis, and D. A. Hutchins, "The use of pulse compression and frequency modulated continuous wave to improve ultrasonic non destructive evaluation of highly-scattering materials," in *Proc. IEEE Int. Ultrason. Symp. IUS*, 2014, pp. 1940–1943, doi: 10.1109/ULTSYM.2014.0482.

[21] T. Isogawa *et al.*, "Tomographic imaging using photonically generated low-coherence terahertz noise sources," *IEEE Trans. Terahertz Sci. Technol.*, vol. 2, no. 5, pp. 485–492, 2012, doi: 10.1109/TTHZ.2012.2208745.

[22] T. Nagatsuma, T. Ikeo, and H. Nishii, "Terahertz imaging based on optical coherence tomography," *Photon. Res,* vol. 2, no. 4, pp. 64–69, 2014, doi: 10.1109/ICECom.2013.6684745.

[23] H. Momiyama, Y. Sasaki, I. Yoshimine, S. Nagano, T. Yuasa, and C. Otani, "Improvement of the depth resolution of swept-source THz-OCT for non-destructive inspection," *Opt. Exp.*, vol. 28, no. 8, pp. 12279, 2020, doi: 10.1364/oe.386680.

[24] C. Am Weg, W. Von Spiegel, R. Henneberger, R. Zimmermann, T. Loeffler, and H. G. Roskos, "Fast active THz cameras with ranging capabilities," *J. Infrared, Millimeter, Terahertz Waves*, vol. 30, no. 12, pp. 1281–1296, 2009, doi: 10.1007/s10762-009-9565-8.

[25] A. Mostajeran, H. Aghasi, S. M. H. Naghavi, and E. Afshari, "Fully integrated solutions for high resolution terahertz imaging (Invited)," in *Proc. Cust. Integr. Circuits Conf.*, 2019, pp. 1–8, doi: 10.1109/CICC.2019.8780262.

[26] T. Nagatsuma *et al.*, "Terahertz wireless communications based on photonics technologies," *Opt. Exp.*, vol. 21, no. 20, pp. 23736, 2013, doi: 10.1364/oe.21.023736.

[27] M. S. Heimbeck and H. O. Everitt, "Terahertz digital holographic imaging," *Adv. Opt. Photon.*, vol. 12, no. 1, p. 1, 2020, doi: 10.1364/aop.12.000001.

[28] L. Rong *et al.*, "Terahertz in-line digital holography of dragonfly hindwing: Amplitude and phase reconstruction at enhanced resolution by extrapolation," *Opt. Exp.*, vol. 22, no. 14, pp. 17236, 2014, doi: 10.1364/oe.22.017236.

[29] D. Damyanov, A. Batra, B. Friederich, T. Kaiser, T. Schultze, and J. C. Balzer, "High-Resolution long-range THz imaging for tunable continuous-wave systems," *IEEE Access*, vol. 8, pp. 151997–152007, 2020, doi: 10.1109/ACCESS.2020.3017821.

[30] O. Monserrat, M. Crosetto, and G. Luzi, "A review of ground-based SAR interferometry for deformation measurement," *ISPRS J. Photogramm. Remote Sens.*, vol. 93, pp. 40–48, 2014, doi: 10.1016/j.isprsjprs.2014.04.001.

[31] T. Löffler, V. Krozer, V. Zhurbenko, A. Kusk, J. Dall, and T. Jensen, "Millimeter-wave imaging systems with aperture synthesis techniques," in *EuCAP 2010 - 4th Eur. Conf. Antennas Propag.*, 2010, pp. 2027–2039.

[32] S. E. Hosseininejad *et al.*, "Reprogrammable Graphene-based metasurface mirror with adaptive focal point for THz imaging," *Sci. Rep.*, vol. 9, no. 1, pp. 1–9, 2019, doi: 10.1038/s41598-019-39266-3.

[33] S. Fan *et al.*, "Diffraction-limited real-time terahertz imaging by optical frequency up-conversion in a DAST crystal," *Opt. Exp.*, vol. 23, no. 6, pp. 7611, 2015, doi: 10.1364/oe.23.007611.

[34] A. Phys, "Real-time terahertz imaging through self- mixing in a quantum-cascade laser," vol. 011102, Jun. 2016, doi: 10.1063/1.4955405.

[35] G. Ok, K. Park, H. S. Chun, H.-J. Chang, N. Lee, and S.-W. Choi, "High-performance sub-terahertz transmission imaging system for food inspection," *Biomed. Opt. Exp.*, vol. 6, no. 5, pp. 1929, 2015, doi: 10.1364/boe.6.001929.

[36] R. A. Lewis, "A review of terahertz detectors," *J. Phys. D. Appl. Phys.*, vol. 52, no. 43, 2019, doi: 10.1088/1361-6463/ab31d5.

[37] A. Rogalski and F. Sizov, "Terahertz detectors and focal plane arrays," *Opto-Electron. Rev,* vol. 19, no. 3, pp. 346–404, 2011, doi: 10.2478/s11772-011-0033-3.

[38] N. Oda *et al.*, "Microbolometer terahertz focal plane array and camera with improved sensitivity in the sub-terahertz region," *J. Infrared, Millimeter, Terahertz Waves*, vol. 36, no. 10, pp. 947–960, 2015, doi: 10.1007/s10762-015-0184-2.

[39] T. J. Smith, A. Broome, D. Stanley, J. Westberg, G. Wysocki, and K. Sengupta, "A hybrid THz imaging system with a 100-Pixel CMOS imager and a 3.25-3.50 THz quantum cascade laser frequency comb," *IEEE Solid-State Circuits Lett.,* vol. 2, no. 9, pp. 151–154, 2019, doi: 10.1109/LSSC.2019.2933332.

[40] T. Sagisaka *et al.*, "Integrated terahertz optics with effective medium for 600-GHz-band imaging," in *Proc. 2020 Int. Topical Meeting Microw. Photon. (MWP)*, 2020, pp. 62–65, doi: 10.23919/MWP48676.2020.9314570.

[41] L. Yi, R. Kaname, Y. Nishida, X. Yu, M. Fujita, and T. Nagatsuma, "Imaging applications with a single resonant tunneling diode transceiver in 300-GHz band," in *Proc. 2020 Int. Topical Meeting Microw. Photon. (MWP)*, 2020, pp. 120–123, doi: 10.23919/MWP48676.2020.9314482.

[42] R. Kaname, T. Sagisaka, L. Yi, and T. Nagatsuma, "600-GHz-Band Terahertz imaging system using frequency-independent concave mirror," in *Proc. 2020 Int. Topical Meeting Microw. Photon. (MWP)*, 2020, pp. 58–61, doi: 10.23919/MWP48676.2020.9314504.

[43] H. D. Qiao, H. Liu, J. C. Mou, and X. Lv, "220 GHz focal plane imaging demonstration using integrated terahertz array detector," *Microw. Opt. Technol. Lett.*, vol. 62, no. 9, pp. 2826–2829, 2020, doi: 10.1002/mop.32388.

[44] A. V. S. P. A. Gusikhin and V. M. M. G. E. Tsydynzhapov, "New ultra-fast sub-terahertz linear scanner," *J. Infrared Millim. Terahertz Waves*, vol. 41, pp. 655–664, 2020.

[45] S.-P. Han *et al.*, "InGaAs schottky barrier diode array detector for a real-time compact terahertz line scanner," *Opt. Exp.*, vol. 21, no. 22, pp. 25874, 2013, doi: 10.1364/oe.21.025874.

[46] Q. Song, Y. Zhao, A. Redo-Sanchez, C. Zhang, and X. Liu, "Fast continuous terahertz wave imaging system for security," *Opt. Commun.*, vol. 282, no. 10, pp. 2019–2022, 2009, doi: 10.1016/j.optcom.2009.02.019.

[47] T. Miyamoto, A. Yamaguchi, and T. Mukai, "Terahertz imaging system with resonant tunneling diodes," *Jpn. J. Appl. Phys.*, vol. 55, no. 3, 2016, doi: 10.7567/JJAP.55.032201.

[48] G. Luzi, M. Crosetto, and E. Fernández, "Radar interferometry for monitoring the vibration characteristics of buildings and civil structures: Recent case studies in spain," *Sensors (Switzerland)*, vol. 17, no. 4, 2017, doi: 10.3390/s17040669.

[49] K. S. Choi, D. R. Utomo, and S. G. Lee, "A fully integrated 490-GHz cmos heterodyne imager adopting second subharmonic resistive mixer structure," *IEEE Microw. Wireless Compon. Lett.*, vol. 29, no. 10, pp. 673–676, 2019, doi: 10.1109/LMWC.2019.2936685.

[50] D. Čibiraitė-Lukenskienė, K. Ikamas, T. Lisauskas, V. Krozer, H. G. Roskos, and A. Lisauskas, "Passive detection and imaging of human body radiation using an uncooled field-effect transistor-based THZ detector," *Sensors (Switzerland)*, vol. 20, no. 15, pp. 1–14, 2020, doi: 10.3390/s20154087.

[51] P. Hillger *et al.*, "A 128-pixel system-on-a-chip for real-time super-resolution terahertz near-field imaging," *IEEE J. Solid-State Circuits*, vol. 53, no. 12, pp. 3599–3612, 2018, doi: 10.1109/JSSC.2018.2878817.

[52] C. Jiang *et al.*, "A fully integrated 320 GHz coherent imaging transceiver in 130 nm sige BiCMOS," *IEEE J. Solid-State Circuits*, vol. 51, no. 11, pp. 2596–2609, 2016, doi: 10.1109/JSSC.2016.2599533.

[53] A. Mostajeran, A. Cathelin, and E. Afshari, "A 170-GHz fully integrated single-chip FMCW imaging radar with 3-D imaging capability," *IEEE J. Solid-State Circuits*, vol. 52, no. 10, pp. 2721–2734, 2017, doi: 10.1109/JSSC.2017.2725963.

[54] N. Rothbart, H. Richter, M. Wienold, L. Schrottke, H. T. Grahn, and H. W. Hubers, "Fast 2-D and 3-D terahertz imaging with a quantum-cascade laser and a scanning mirror," *IEEE Trans. Terahertz Sci. Technol.*, vol. 3, no. 5, pp. 617–624, 2013, doi: 10.1109/TTHZ.2013.2273226.

[55] A. Nakanishi, K. Fujita, K. Horita, and H. Takahashi, "Terahertz imaging with room-temperature terahertz difference-frequency quantum-cascade laser sources," *Opt. Exp.*, vol. 27, no. 3, pp. 1884, 2019, doi: 10.1364/oe.27.001884.

[56] M. C. Wanke *et al.*, "Monolithically integrated solid-state terahertz transceivers," *Nat. Photon.*, vol. 4, no. 8, pp. 565–569, 2010, doi: 10.1038/nphoton.2010.137.

[57] H. Song, S. Hwang, H. An, H.-J. Song, and J.-I. Song, "Continuous-wave THz vector imaging system utilizing two-tone signal generation and self-mixing detection," *Opt. Exp.*, vol. 25, no. 17, pp. 20718, 2017, doi: 10.1364/oe.25.020718.

[58] S. Preu, G. H. Dhler, S. Malzer, L. J. Wang, and A. C. Gossard, "Tunable, continuous-wave terahertz photomixer sources and applications," *J. Appl. Phys.*, vol. 109, no. 6, 2011, doi: 10.1063/1.3552291.

[59] D.-S. Yee, J. S. Yahng, C.-S. Park, H. D. Lee, and C.-S. Kim, "High-speed broadband frequency sweep of continuous-wave terahertz radiation," *Opt. Exp.*, vol. 23, no. 11, pp. 14806, 2015, doi: 10.1364/oe.23.014806.

[60] T. Ishibashi and H. Ito, "Uni-traveling-carrier photodiodes," *J. Appl. Phys.*, vol. 127, no. 3, 2020, doi: 10.1063/1.5128444.

[61] A. Tessmann *et al.*, "A 600 GHz low-noise amplifier module," *IEEE MTT-S Int. Microw. Symp. Dig.*, pp. 0–2, 2014, doi: 10.1109/MWSYM.2014.6848456.

[62] E. N. Grossman, K. Leong, X. Mei, and W. Deal, "Low-frequency noise and passive imaging with 670 GHz HEMT low-noise amplifiers," *IEEE Trans. Terahertz Sci. Technol.*, vol. 4, no. 6, pp. 749–752, 2014, doi: 10.1109/TTHZ.2014.2352035.

[63] D. Cibiraite *et al.*, "TeraFET multi-pixel THz array for a confocal imaging system," *Int. Conf. Infrared, Millimeter, Terahertz Waves, IRMMW-THz*, 2019, pp. 2–3, doi: 10.1109/IRMMW-THz.2019.8874217.

[64] J. W. Holloway, G. C. Dogiamis, and R. Han, "Innovations in terahertz interconnects: High-speed data transport over fully electrical terahertz waveguide links," *IEEE Microw. Mag.*, vol. 21, no. 1, pp. 35–50, Jan. 2020, doi: 10.1109/MMM.2019.2945139.

[65] K. Murano *et al.*, "Low-Profile terahertz radar based on broadband leaky-wave beam steering," *IEEE Trans. Terahertz Sci. Technol.*, vol. 7, no. 1, pp. 60–69, 2017, doi: 10.1109/TTHZ.2016.2624514.

[66] K. Tsuruda, M. Fujita, and T. Nagatsuma, "Extremely low-loss terahertz waveguide based on silicon photonic-crystal slab," *Opt. Exp.*, vol. 23, no. 25, pp. 31977, 2015, doi: 10.1364/oe.23.031977.

[67] D. Headland, M. Fujita, and T. Nagatsuma, "Half-Maxwell fisheye lens with photonic crystal waveguide for the integration of terahertz optics," *Opt. Exp.*, vol. 28, no. 2, pp. 2366, 2020, doi: 10.1364/oe.381809.

[68] D. Headland, X. Yu, M. Fujita, and T. Nagatsuma, "Near-field vertical coupling between terahertz photonic crystal waveguides," *2019 URSI Asia-Pacific Radio Sci. Conf. AP-RASC 2019*, vol. 6, no. 8, 2019, doi: 10.23919/URSIAP-RASC.2019.8738435.

[69] M. Wienold *et al.*, "Real-time terahertz imaging through self-mixing in a quantum-cascade laser," *Appl. Phys. Lett.*, vol. 109, no. 1, 2016, doi: 10.1063/1.4955405.

[70] J. Grajal *et al.*, "Compact radar front-end for an imaging radar at 300 GHz," *IEEE Trans. Terahertz Sci. Technol.*, vol. 7, no. 3, pp. 268–273, 2017, doi: 10.1109/TTHZ.2017.2673544.

[71] M. Asada and S. Suzuki, "Terahertz oscillators using electron devices - an approach with resonant tunneling diodes," *IEICE Electron. Exp.*, vol. 8, no. 14, pp. 1110–1126, 2011, doi: 10.1587/elex.8.1110.

[72] T. Maekawa, H. Kanaya, S. Suzuki, and M. Asada, "Oscillation up to 1.92 THz in resonant tunneling diode by reduced conduction loss," *Appl. Phys. Exp.*, vol. 9, no. 2, 2016, doi: 10.7567/APEX.9.024101.

[73] Y. Takida, S. Suzuki, M. Asada, and H. Minamide, "Sensitive terahertz-wave detector responses originated by negative differential conductance of resonant-tunneling-diode oscillator," *Appl. Phys. Lett.*, vol. 117, no. 2, 2020, doi: 10.1063/5.0012318.

[74] Y. Nishida, N. Nishigami, S. Diebold, J. Kim, M. Fujita, and T. Nagatsuma, "Terahertz coherent receiver using a single resonant tunnelling diode," *Sci. Rep.*, vol. 9, no. 1, pp. 1–3, 2019, doi: 10.1038/s41598-019-54627-8.

[75] H. Chang, "Phase noise in self-injection-locked oscillators — Theory and experiment," in *IEEE Trans. Microw. Theory Techn.*, vol. 51, no. 9, pp. 1994–1999, Sep. 2003.

[76] B. Razavi, "A study of injection locking and pulling in oscillators," *IEEE J. Solid-State Circuits*, vol. 39, no. 9, pp. 1415–1424, Sep. 2004, doi: 10.1109/JSSC.2004.831608.

[77] M. Asada and S. Suzuki, "Theoretical analysis of external feedback effect on oscillation characteristics of resonant-tunneling-diode terahertz oscillators," *Jpn. J. Appl. Phys.*, vol. 54, no. 7, pp. 18–21, 2015, doi: 10.7567/JJAP.54.070309.

[78] Z. H. Zhai *et al.*, "Design of terahertz-wave doppler interferometric velocimetry for detonation physics," *Appl. Phys. Lett.*, vol. 116, no. 16, 2020, doi: 10.1063/1.5142415.

[79] N. Oda, "Technology trend in real-time, uncooled image sensors for sub-THz and THz wave detection," *Micro- Nanotechnol. Sensors, Syst. Appl. VIII*, vol. 9836, pp. 98362P, 2016, doi: 10.1117/12.2222290.

[80] J. He, T. Dong, B. Chi, and Y. Zhang, "Metasurfaces for terahertz wavefront modulation : A review," *J. Infrared, Millimeter, Terahertz Waves*, vol. 41, pp. 607–631, 2020.

[81] H. Yi, S. W. Qu, B. J. Chen, X. Bai, K. B. Ng, and C. H. Chan, "Flat terahertz reflective focusing metasurface with scanning ability," *Sci. Rep.*, vol. 7, no. 1, pp. 2–9, 2017, doi: 10.1038/s41598-017-03752-3.

[82] A. D. A. M. V. Allés, J. H. E. Iahuan, S. E. O. Hno, T. Akashige, O. Matsu, and K. A. M. Iyamoto, "Broadband high-resolution terahertz single-pixel imaging," vol. 28, no. 20, pp. 28868–28881, 2020.

[83] R. I. Stantchev, X. Yu, T. Blu, and E. Pickwell-MacPherson, "Real-time terahertz imaging with a single-pixel detector," *Nat. Commun.*, vol. 11, no. 1, pp. 1–8, 2020, doi: 10.1038/s41467-020-16370-x.

[84] K. H. Jin, Y.-G. Kim, S. H. Cho, J. C. Ye, and D.-S. Yee, "High-speed terahertz reflection three-dimensional imaging for nondestructive evaluation," *Opt. Exp.*, vol. 20, no. 23, pp. 25432, 2012, doi: 10.1364/oe.20.025432.

[85] Y. Kujime, M. Fujita, and T. Nagatsuma, "Terahertz tag using photonic-crystal slabs," *J. Light. Technol.*, vol. 36, no. 19, pp. 4386–4392, 2018, doi: 10.1109/JLT.2018.2825464.

[86] E. S. Lee *et al.*, "Semiconductor-Based terahertz photonics for industrial applications," *J. Light. Technol.*, vol. 36, no. 2, pp. 274–283, 2018, doi: 10.1109/JLT.2017.2786260.

[87] K. B. Cooper *et al.*, "Fast high-resolution terahertz radar imaging at 25 meters," *Terahertz Phys., Devices, Syst. IV Adv. Appl. Ind. Def.*, vol. 7671, p. 76710Y, Apr. 2010, doi: 10.1117/12.850395.

[88] A. García-Pino, N. Llombart, B. Gonzalez-Valdes, and O. Rubiños-López, "A Bifocal ellipsoidal Gregorian reflector system for THz imaging applications," *IEEE Trans. Antennas Propag.*, vol. 60, no. 9, pp. 4119–4129, Sep. 2012, doi: 10.1109/TAP.2012.2207064.

[89] X. Gao, C. Li, S. Gu, and G. Fang, "Design, analysis and measurement of a millimeter wave antenna suitable for stand off imaging at checkpoints," *J. Infrared, Millimeter, Terahertz Waves*, vol. 32, no. 11, pp. 1314–1327, 2011, doi: 10.1007/s10762-011-9825-2.

[90] S. Gu, C. Li, X. Gao, Z. Sun, and G. Fang, "Terahertz aperture synthesized imaging with fan-beam scanning for personnel screening," *IEEE Trans. Microw. Theory Tech.*, vol. 60, no. 12, pp. 3877–3885, 2012, doi: 10.1109/TMTT.2012.2221738.

[91] N. Llombart, K. B. Cooper, R. J. Dengler, T. Bryllert, and P. H. Siegel, "Confocal ellipsoidal reflector system for a mechanically scanned active terahertz imager," *IEEE Trans. Antennas Propag.*, vol. 58, no. 6, pp. 1834–1841, 2010, doi: 10.1109/TAP.2010.2046860.

[92] L. D. Manh *et al.*, "External feedback effect in terahertz resonant tunneling diode oscillators," *IEEE Trans. Terahertz Sci. Technol.*, vol. 8, no. 4, pp. 455–464, 2018, doi: 10.1109/TTHZ.2018.2842209.

[93] T. Hiraoka *et al.*, "Injection locking and noise reduction of resonant tunneling diode terahertz oscillator," *APL Photon.*, vol. 6, no. 2, 2021, doi: 10.1063/5.0033459.

[94] M. Ljubenovic, L. Zhuang, J. De Beenhouwer, and J. Sijbers, "Joint deblurring and denoising of THz time-domain images," *IEEE Access*, vol. 9, pp. 162–176, 2021, doi: 10.1109/ACCESS.2020.3045605.

[95] B. Baccouche *et al.*, "Three-Dimensional terahertz imaging with sparse multistatic line arrays," *IEEE J. Sel. Topics Quantum Electron.*, vol. 23, no. 4, 2017, doi: 10.1109/JSTQE.2017.2673552.

Li Yi (Member, IEEE) received the B.Sc. degree in geophysics from the School of Ocean and Earth Science, Tongji University, Shanghai, China, in 2011, and the M.E. and Ph.D. degrees in environmental studies from the Graduate School of Environmental Studies, Tohoku University, Sendai, Japan, in 2014 and 2017, respectively. Then he was a Researcher of the National Institute of Advanced Industrial Science and Technology(AIST) until 2018.

He is currently an Assistant Professor with the Graduate School of Engineering Science, Osaka University, Suita, Japan. His research interests include photonic based millimeter or terahertz waves devices and applications, which include imaging and sensing techniques, wireless communication, and signal processing techniques. He is a Member of the Institute of Electronics, Information and Communication Engineers (IEICE), Japan. He is currently an Associate Editor for the *IEICE Electronics Express*.

He was the recipient of the Student Paper Competition Prize of URSI Japan Radio Science Meeting 2015 and was awarded the President Award of environmental study of Tohoku University in 2017, and the Young Scientists Award of IEICE, SANE in 2018.

Yosuke Nishida received the B.E. and M.E. degrees in engineering science from Osaka University, Osaka, Japan, in 2016 and 2018, respectively. In 2018, he joined ROHM Co., Ltd., Kyoto, Japan. His research interests include terahertz integrated circuits for imaging and wireless communication applications based on resonant tunneling diodes.

Tomoki Sagisaka received the B.E. and M.E. degrees in engineering science from Osaka University, Osaka, Japan, in 2019 and 2021, respectively. In 2021, he joined Sony Semiconductor Solutions Corporation, Kanagawa, Japan. His research interests include system development and integration for terahertz imaging and sensing applications.

Ryohei Kaname (Member, IEEE) received the B.E. degree in 2020 in engineering science from Osaka University, Osaka, Japan, where he is currently working toward the M.E. degree. His current research interests include terahertz imaging and sensing and its applications. He is a Member of the Institute of Electronics, Information and Communication Engineers (IEICE), Japan.

Ryoko Mizuno received the B.E. degree in 2021 in engineering science from Osaka University, Osaka, Japan, where she is a first year master student, studying under Professor Tadao Nagatsuma.. Her research focuses on terahertz imaging by using resonant tunneling diode transceiver.

Masayuki Fujita (Member, IEEE) received the Ph.D. degree from Yokohama National University, Yokohama, Japan, on ultrasmall and ultralow-threshold microdisk lasers, in 2002. Subsequently, he joined the Department of Electronic Science and Engineering, Kyoto University, Kyoto, Japan, and initiated research on photonic crystals, including spontaneous emission control in photonic crystals and high-efficiency light extraction in light-emitting diodes and silicon light emitters. Next, he moved to Osaka University, Osaka, Japan, and was appointed the Research Director of the strategic basic research program CREST, "development of terahertz integrated technology platform through fusion of resonant tunneling diodes and photonic crystals" of the Japan Science and Technology Agency.

He is currently an Associate Professor with the Graduate School of Engineering Science, Osaka University, Toyonaka, Japan. His research interests include terahertz materials and devices, photonic nanostructures and microstructures, and their applications. He is a Member of the Japan Society of Applied Physics (JSAP), the Laser Society of Japan, the Institute of Electronics, Information and Communication Engineers, Japan, and the Japanese Photochemistry Association. From 1999 to 2002 and from 2003 to 2006, he was a Research Fellow of the Japan Society for the Promotion of Science (JSPS). He is currently an Associate Editor for the *Applied Physics Express*, and the Chair of the Technical Group on Terahertz Application Systems of Information and Communication Engineers (IEICE), Japan.

Tadao Nagatsuma (Fellow, IEEE) received the B.S., M.S., and Ph.D. degrees in electronic engineering from Kyushu University, Fukuoka, Japan, in 1981, 1983, and 1986, respectively. In 1986, he joined the Electrical Communications Laboratories, Nippon Telegraph and Telephone Corporation (NTT), Atsugi, Kanagawa, Japan. From 1999 to 2002, he was a Distinguished Technical Member with NTT Telecommunications Energy Laboratories. From 2003 to 2007, he was a Group Leader with NTT Microsystem Integration Laboratories and was a NTT Research Professor from 2007 to 2009. Since 2007, he has been with Osaka University, Osaka, Japan, where he is currently a Professor with the Division of Advanced Electronics and Optical Science, Department of Systems Innovation, Graduate School of Engineering Science. His research interests include ultrafast electronics and millimeter-wave and terahertz photonics.

He is a Fellow of the Institute of Electronics, Information and Communication Engineers (IEICE), Japan, and a Fellow of the Electromagnetics Academy. He is currently an Associate Editor for the IEEE Photonics Technology Letters and the IEEE TRANSACTIONS ON TERAHERTZ SCIENCE AND TECHNOLOGY, and the Vice President of the IEICE and the Terahertz Systems Consortium. He was the recipient of numerous awards, including the 1989 IEICE Young Engineers Award, the 1992 IEEE Andrew R. Chi Best Paper Award, the 1997 Okochi Memorial Award, the 1998 Japan Microwave Prize, the 2000 Ministers Award of the Science and Technology Agency, the 2002 and 2011 Asia–Pacific Microwave Conference Prize, the 2004 YRP (Yokosuka Research Park) Award, the 2006 Asia–Pacific Microwave Photonics Conference Award, the 2006 European Microwave Conference Prize, the 2007 Achievement Award presented by the IEICE, the 2008 Maejima Award, the 2011 Recognition from Kinki Bureau of Telecommunications, Ministry of Internal Affairs and Communications, the 2011 Commendation for Science and Technology by the Ministry of Education, Culture, Sports, Science and Technology, and the 2014 IEEE Tatsuo Ito Award, and the 2020 Distinguished Achievement and Contributions Award by the IEICE.